THE BACTERIAL RIBOSOME AS A TARGET FOR ANTIBIOTICS

Jacob Poehlsgaard and Stephen Douthwaite

Abstract | Many clinically useful antibiotics exert their antimicrobial effects by blocking protein synthesis on the bacterial ribosome. The structure of the ribosome has recently been determined by X-ray crystallography, revealing the molecular details of the antibiotic-binding sites. The crystal data explain many earlier biochemical and genetic observations, including how drugs exercise their inhibitory effects, how some drugs in combination enhance or impede each other's binding, and how alterations to ribosomal components confer resistance. The crystal structures also provide insight as to how existing drugs might be derivatized (or novel drugs created) to improve binding and circumvent resistance.

Department of Biochemistry & Molecular Biology, University of Southern Denmark, DK-5230 Odense M, Denmark.
Correspondence to S.D.
e-mail: srd@bmb.sdu.dk
doi:10.1038/nrmicro1265
Published online
2 October 2005

The ribosome is nature's largest and most complex enzyme, consisting, even in the simplest organisms, of more than fifty different protein and RNA components with a total mass of over two million daltons. The ribosome is also nature's most ancient enzyme, and carries out the same essential function (the manufacture of new proteins) in all living cells. This preservation of function has been coupled with an overall conservation of structure, and ribosomes in organisms as phylogenetically distinct as bacteria and archaea show a remarkable degree of resemblance. Furthermore, present evidence indicates that eukaryotic ribosomes, including those in human cells, are also similar in structure to their prokaryotic counterparts. The last time these organisms shared a common living relative was about three and a half billion years ago, and during the intervening period there have been many substitutions in the sequences of the component ribosomal proteins (r-proteins) and ribosomal RNAs (rRNAs) and, admittedly, the human cytoplasmic ribosomes have put on some extra mass (TABLE 1). However, despite the sequence changes, the overall tertiary folds of the ribosomal components and the manner in which they fit together have been retained over the course of evolution. This conservation of structure is most evident in the regions of the ribosome that are directly engaged in the functional steps of protein synthesis (BOX 1).

The ribosome is therefore a complex system made up of interdependent components that require a particular arrangement to function. As in other complex systems, loss of function can be brought about in a multitude of ways by disrupting the optimal arrangement of the component parts (as anyone who has tried poking a screwdriver into their computer will know). In a rather more subtle manner, this is what ribosome-targeting antibiotics do — they lodge between crucial components, disrupting the manner in which they operate and thereby interfering with the synthesis of new proteins. Many chemically diverse antibiotic compounds act in this way and, as can be seen in FIG. 1, they target the ribosome at surprisingly few locations, which results in overlap between many of their binding sites. A clear picture of how many of these antibiotics recognize their binding sites has become available recently with the atomic-level structures of the ribosome obtained by X-ray crystallography. The antibiotic sites tend to be at the mechanistically active regions on the ribosome structure, which we describe below before reviewing the details of antibiotic action.

Elucidating the structure of the ribosome

The discovery of the ribosome's central role in protein synthesis in the 1950s was the starting point of intensive research into how this ribonucleoprotein complex translates genetic information into proteins, and how

this process is blocked by so many antibiotics[1–4]. As in other fields of molecular biology, *Escherichia coli* became the standard model for ribosome studies, with useful supplementary information derived from other bacteria and yeast. An overview of the components in ribosomes from the different domains of life is given in TABLE 1.

The overall shape and dimensions of the ribosome were first visualized by electron microscopy[5–7], and this discipline was later refined with cryo-techniques[8,9] so that the ribosome could be captured at various stages of translation[10–12]. Considerable contributions were also made by biochemical and genetic approaches, and these led to a gradual shift in the perception of the relative roles of the ribosomal components. Originally, the RNA components of the ribosome were regarded as mere scaffolding for the (presumed) catalytically active r-proteins, and this view has now been superseded by one in which the rRNAs are the key players in ribosome function, with the r-proteins acting in supporting roles. This latter view had long been held by several researchers in the field, and many data were tantalizingly indicative of the rRNA-catalyst model[13,14], while falling somewhat short of being entirely conclusive. RNA molecules that were transcribed *in vitro* were selected for their ability to catalyse peptide-bond formation[15], and this added weight to the argument that protein synthesis by the ribosome was also catalysed by RNA. However, the most compelling evidence came at the end of the twentieth century with the high-resolution structures obtained from X-ray diffraction analyses of ribosome crystals. At the site of peptide-bond formation on the 50S subunit (the peptidyl-transferase centre), no r-protein is closer than 18 Å (REF. 16) and, barring any gross rearrangements of r-proteins in the crystal structure, this more or less rules out that peptide-bond formation can be anything other than RNA-directed.

Table 1 | **Ribosome components from the three domains of life**

Characteristics	Bacteria	Archaea	Mitochondria	Eukarya
Ribosome size	70S	70S	55S	80S
Small subunit				
Size	30S	30S	28S	40S
Mass (MDa)	0.8	0.8	1.2	1.4
rRNAs	16S	16S	12S	18S
Number of r-proteins	20	28	33	32
Large subunit				
Size	50S	50S	39S	60S
Mass (MDa)	1.6	1.6	2.4	2.6
rRNAs	23S, 5S	23S, 5S	16S	28S, 5.8S, 5S
Number of r-proteins	34	40	52	46

Ribosomes from all domains of life function in essentially the same manner. Bacterial and archaeal ribosomes are approximately the same size, whereas the ribosomes in Eukarya are much larger. Differences in rRNA and r-protein components allow antibiotics and cytotoxins to exhibit specificity for the ribosomes of one domain. Chloroplast ribosomes (not shown) are structurally closest to the bacterial domain. Mitochondrial ribosomes (based on the rat genome sequence) have evolved away from the other structures, including their cytoplasmic counterparts, and contain a larger complement of r-proteins relative to the rRNA.

The present evidence indicates that the rRNA aligns the aminoacyl and peptidyl moieties on the aminoacyl site (A site) and peptidyl site (P site) transfer RNAs (tRNAs) in an optimal configuration for peptide-bond formation[17–19]. The exact mechanism of this process is still under debate, but undoubtedly involves the universally conserved nucleotide A2451 (REFS 16,20,21).

Crystallization of the ribosome. Crystals of ribosomes suitable for structural studies were first reported two decades ago[22–25] and since then, collection and interpretation of highly resolved X-ray diffraction patterns has occurred together with advances on several technological fronts. Notably, these included the use of cryo-techniques to stabilize crystals in the powerful synchrotron beams, the development of high-speed detectors, the means of determining phase angles, and the rapidly expanding capacity of computers[18,26].

All ribosomes have a large asymmetric structure, and the organism from which they are isolated is an important consideration for obtaining suitable crystals. Ribosomes from *Thermus thermophilus*, a bacterium that grows optimally at about 70°C, form particularly good crystals, and these have been used by laboratories in Salt Lake City, USA and Cambridge, England[27] and in Hamburg, Germany and Rehovot, Israel[28] to determine the structure of the small ribosomal subunit at a resolution of around 3 Å. The structure of the entire ribosome of *T. thermophilus* was also solved in Santa Cruz, California[29], and although the resolution is lower, these crystals provide valuable additional information about how the two subunits associate to accommodate the messenger RNA (mRNA) together with the tRNAs[30] (BOX 1). The best resolution so far (at 2.4 Å) has been obtained using crystals of the large ribosomal subunit from *Haloarcula marismortui*, an archaeon from the Dead Sea in Israel that grows optimally in saturated salt solutions[31]. The bacterium *Deinococcus radiodurans*, notorious for its resilience to radiation sterilization in the food-canning process, has also proven a source of stable ribosomes that yield highly resolved diffraction patterns[32].

All the above organisms live under arduous conditions, and this is reflected in the natural robustness of their ribosomes, which can withstand crystallographic analysis. However, these organisms are evolutionarily far removed from the bacterial strains normally used in the laboratory or those causing disease. Although the phylogenetic conservation of the ribosome's shape and function to a great extent allays doubt about the general applicability of these structures, it is nevertheless comforting that 70S ribosomes from the faithful workhorse *E. coli* have now been crystallized[33]. The published resolution of the structure is presently relatively low at around 10 Å but, as far as can be gleaned from these data, the ribosomes in *Escherichia* are reassuringly similar to those in *Deinococcus*, *Haloarcula* and *Thermus*. Higher-resolution data on the *E. coli* ribosome are anticipated soon and will provide an important link with the comprehensive biochemical and genetic studies on this bacterium.

Box 1 | **Protein synthesis by the ribosome**

Ribosomes translate the genetic information encoded in messenger RNA (mRNA) to assemble amino acids into proteins. Ribosomes are made up of two subunits, both of which consist of ribosomal RNA (rRNA) and many proteins (r-proteins). In the upper panel of the figure, the backbone traces of the rRNAs (yellow and grey) and the r-proteins (bronze and blue) are shown at the interfaces of the small (30S) and large (50S) ribosomal subunits from the thermophilic bacterium *Thermus thermophilus*. The small subunit contains the decoding site where the mRNA sequence (magenta) is read in blocks of three nucleotides, called codons. Each codon denotes one of twenty different amino acids, and each amino acid is ferried to the ribosome by its own transfer RNA (tRNA) or set of tRNAs. Every tRNA has an anticodon sequence that makes a specific match with the corresponding mRNA codon. The mRNA passes through two narrow channels on the 30S subunit to be displayed at the interface decoding site, where it interacts with the tRNA anticodon (see figure, lower panel). Protein synthesis is initiated when the start codon on the mRNA is guided into the peptidyl site (P site) on the 30S subunit to interact with the initiator tRNA (green) charged with the amino acid methionine. The interfaces of the small and large subunits then come into contact as shown in the vertical section through the P site (see figure, lower panel). Then, the second mRNA codon, in the adjacent aminoacyl site (A site), accepts the next tRNA with its amino acid. The base-pairing match between the tRNA anticodon and mRNA codon is checked by the decoding site within the A site of the small subunit. If the match is accepted, the aminoacyl end of the tRNA is swung into the catalytic site, the peptidyl-transferase centre, on the large subunit, where a peptide bond is formed between the methionine and the second amino acid. The ribosome then moves one codon along the mRNA, bringing the third codon into the A site; this translocates the tRNA holding the dipeptide into the P site, and the deacylated initiator tRNA is moved into the exit site (E site) from where it is ejected. The cycle is repeated up to several hundred times, and the peptide chain grows from the peptidyl-transferase centre through the tunnel in the large subunit to emerge at the back of the ribosome (red arrow). Eventually the ribosome reaches a stop codon on the mRNA, signalling the completion and release of the peptide chain. All these stages in the initiation, elongation and release of the peptide chain are helped by protein factors, usually with the expenditure of energy in the form of guanosine nucleotide triphosphate (GTP).

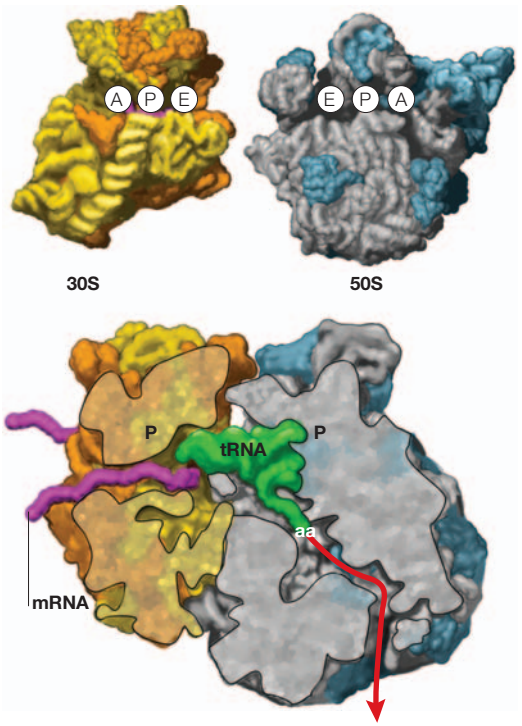

The ribosome's anatomy. The 30S ribosomal subunit is made up of around 50,000 atoms larger than hydrogen, and the 50S subunit has about twice this number of atoms. Now that the enormous task of solving these structures has been accomplished, viewing the data is fairly straightforward if a systematic approach is taken. The ribosome is much larger than other structures solved by nuclear magnetic resonance (NMR) and X-ray crystallography, so not all software packages can handle the quantity of data. For a selection of suitable programs together with hints on their use, see Supplementary information S1 (box).

One feature that is immediately apparent is the scarcity of r-proteins in the 'business' regions of the ribosome at the interfaces of the two subunits (BOX 1). The different crystal models are consistent in showing the same rRNA-rich distribution at the subunit interfaces, strongly indicating that this represents a true picture of all ribosomes. The conspicuous lack of protein in the functional regions begs the question as to what the r-proteins are doing. Many of the r-proteins have globular domains that emerge on the sides and back of the subunits, and some of these r-proteins have elongated subdomains that extend into the body of the subunit to interact with the rRNAs. The r-protein interactions influence the structure of the rRNA, enabling it to adopt conformations that are required for its rapid and efficient function[34–36]. Many of these RNA conformations are thermodynamically unfavourable, and might be difficult, if not impossible, for the rRNAs to attain without the help of the r-proteins. Further functions of the r-proteins include helicase activity to gain access to the information in tightly structured mRNAs as they enter the ribosome[37], gating functions in the peptide tunnel (discussed below)[38–42], and docking sites for chaperones at the tunnel exit site on the back of the ribosome[43]. Therefore, despite the ability of the rRNA components to direct and catalyse peptide-bond formation, the functional repertoire of a ribosome made entirely of RNA would be insufficient to meet the rapid and constantly changing requirements for protein synthesis in a living cell.

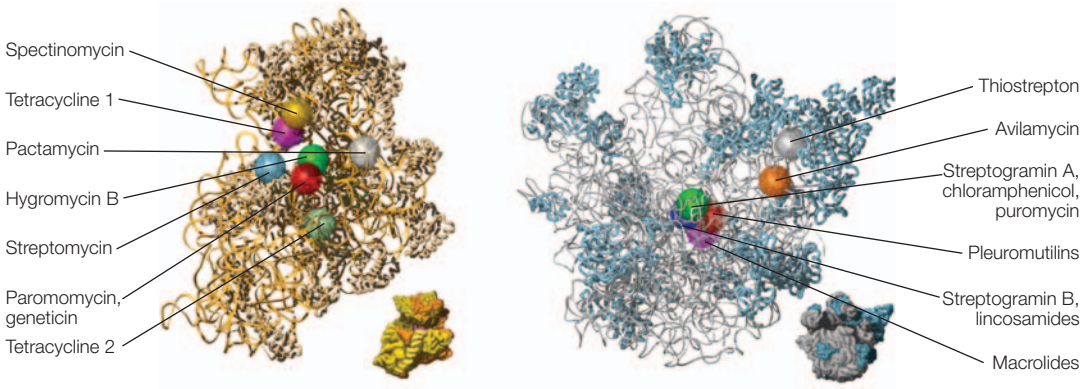

Figure 1 | **Binding sites of antibiotics on the bacterial ribosome.** The 30S ribosomal subunit is shown on the left and the 50S ribosomal subunit is shown on the right. The antibiotic-binding sites were initially determined by biochemical and genetic techniques; subsequently, many sites were revealed in greater detail by X-ray crystallography. At the overlapping sites, antibiotic binding is usually mutually exclusive (for example, for macrolide, lincosamide and streptogramin B compounds), however, streptogramin A and B compounds bind synergistically at adjacent sites. Subunit models are based on the *Thermus thermophilus* 70S ribosome structure[29]. In this figure, for clarity, part of the r-protein L9 has been omitted. Ribosomal RNAs are shown in yellow and grey and r-proteins in bronze and blue.

Antibiotic-binding sites on the ribosome

Given the fundamental importance of the rRNA, it is not surprising that most ribosome inhibitors target the rRNA-rich surfaces on the 30S and 50S subunits (FIG. 1). The crystal structures of many ribosome-targeting antibiotics have been solved in complex with their ribosomal subunit. The 30S subunit is targeted by drugs that include tetracycline, pactamycin and the aminoglycosides (see TABLE 2), which hinder the subunit in carrying out its principle function of deciphering the genetic information encoded in the mRNA (BOX 1). Binding of aminoglycosides such as geneticin, paromomycin (FIG. 2) and apramycin at the decoding site of the 30S subunit have been well studied by NMR[44,45] and crystallography[46–49].

The 50S subunit is targeted by a wide range of drugs that bind within three main regions (FIG. 1) to interfere with the subunit's main functions in controlling GTP hydrolysis, the formation of peptide bonds, and channelling the peptide through the subunit tunnel (BOX 1). Binding of the thiopeptide antibiotics such as thiostrepton inhibit GTP-associated processes[50–52], whereas the oligosaccharide antibiotics avilamycin and evernimicin interrupt a subset of these processes by binding to their own distinct site[53–56]. So far, there are no crystallographic data on the thiopeptide or oligosaccharide compounds bound to their sites on the 50S subunit. Interactions of drugs at the third binding region on the 50S subunit (FIG. 1) have, however, been subject to rigorous crystallographic study. This latter region is extensive, covering the upper part of the tunnel together with the peptidyl-transferase centre, and accommodates a diverse range of drugs, including the MLS_B (macrolide, lincosamide, streptogramin B) compounds[1,2,42,57–60], chloramphenicol[57,59], puromycin[16], pleuromutilins[61,62] and oxazolidinones[63,64].

Below, we concentrate on drug targets at the two main and best-characterized reaction centres in the ribosome — the aminoglycoside target at the decoding site on the 30S subunit, and the target for MLS_B compounds adjacent to the peptidyl-transferase centre in the 50S subunit.

Table 2 | **Antibiotics that target the 30S ribosomal subunit**

Drug	PDB	Resolution (Å)	System	Ref.
Aminoglycosides*				
Streptomycin	1FJG	3.0	*Thermus*	46
Paromomycin	1FJG	3.0	*Thermus*	46
Hygromycin B	1HNZ	3.3	*Thermus*	119
Paromomycin	1IBK	3.3	*Thermus*	66
Paromomycin	1J7T	2.5	RNA fragment	47
Tobramycin	1LC4	2.5	RNA fragment	120
Geneticin	1MWL	2.4	RNA fragment	48
Apramycin	1YRJ	2.7	RNA fragment	121
Tetracyclines‡				
Tetracycline	1HNW	3.4	*Thermus*	119
Tetracycline	1I97	4.5	*Thermus*	122
Cyclic peptides‡				
Viomycin	-	-	nd	-
Capreomycin	-	-	nd	-
Other 30S drugs§				
Edeine	1I95	4.5	*Thermus*	122
Spectinomycin	1FJG	3.0	*Thermus*	46
Pactamycin	1HNX	3.4	*Thermus*	119

*Bind to aminoacyl or peptidyl sites and induce errors in translation. ‡Block binding of transfer RNA to aminoacyl site. §Various effects, including inhibition of translocation. The *Thermus* system refers to 30S subunits from the bacterium *Thermus thermophilus*; RNA fragment contains the decoding region of 16S rRNA. nd, crystal structure not determined; PDB, Protein Data Bank ID.

The decoding site on the 30S subunit

The decoding site is part of the ribosomal A site and is situated at the end of the 16S rRNA helix 44 on the 30S subunit interface (BOX 1). The function of the decoding site is to monitor codon–anticodon pairing after the aminoacylated tRNA has been placed in the

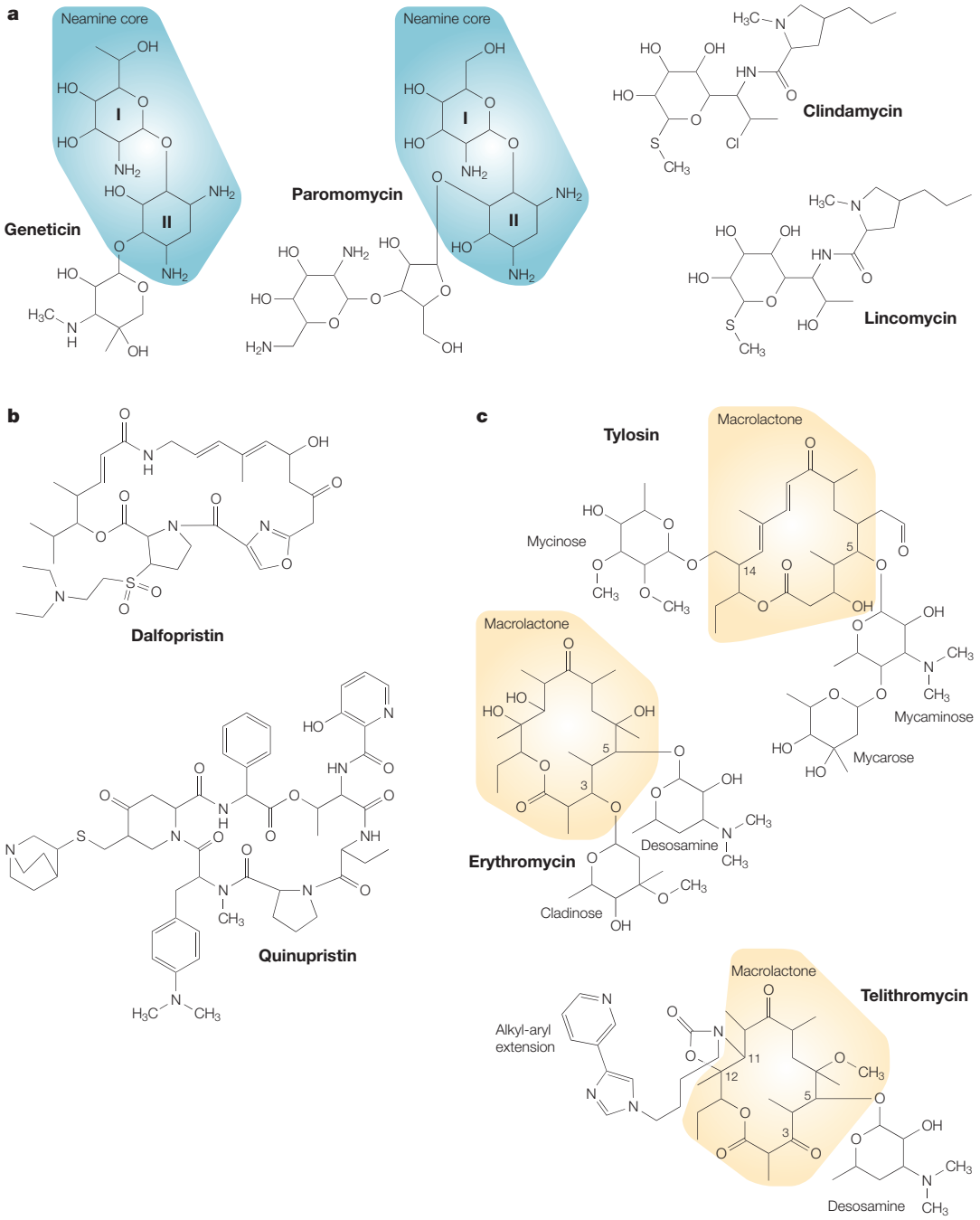

Figure 2 | **Chemical structures of a selection of ribosome-targeting drugs. a** | Geneticin and paromomycin are aminoglycosides, and their common neamine structure (rings I and II) is highlighted. Clindamycin is a derivative of the lincosamide antibiotic lincomycin. **b** | Dalfopristin and quinupristin are streptogramin A and B compounds, respectively. **c** | Erythromycin and tylosin are naturally occurring macrolides, with 14- and 16-membered macrolactone rings, respectively (highlighted) and different sugar residues. Telithromycin is a ketolide antibiotic (so-called because the cladinose sugar at the 3-position has been substituted by a keto-group), and is one of the latest semi-synthetic derivatives of erythromycin.

A site by elongation factor Tu complexed with GTP. Within the decoding site, two universally conserved nucleotides, A1492 and A1493, are essential for the monitoring process, particularly at the first two bases of the codon[65,66]. When there is a cognate fit between the mRNA codon and the tRNA anticodon, their ribose–phosphate backbone adopts a geometry that favours hydrogen bonding with the bases of nucleotides A1492 and A1493. To engage in this interaction, A1492 and A1493 must first flip out of helix 44 into the conformation illustrated in FIG. 3. Binding of tRNA to the A site is also accompanied by other changes in

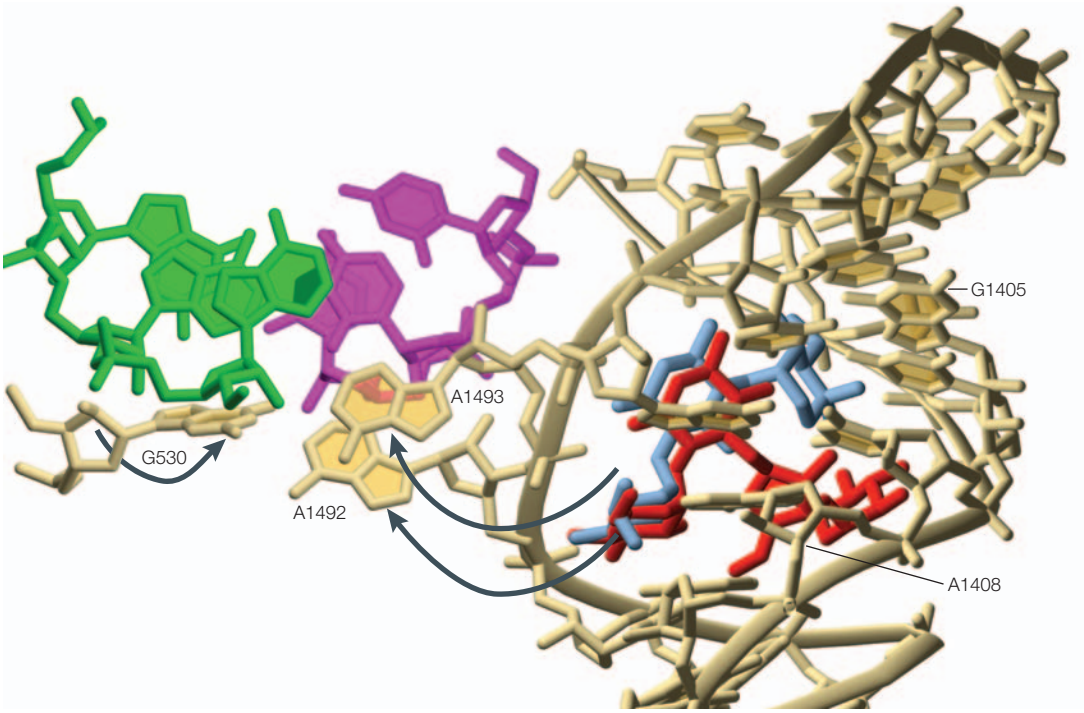

Figure 3 | **The decoding site at the interface of the 30S ribosomal subunit.** Nucleotides A1492 and A1493 are shown in the conformation that they adopt after having flipped out of the 16S rRNA helix 44 to interact with an mRNA codon (magenta) and its cognate tRNA anticodon (green) at the ribosomal aminoacyl site[66]. The conformational changes induced at these nucleotides and at G530 are indicated by the arrows. The aminoglycoside antibiotics paromomycin (red) and geneticin (blue) bind within helix 44 as shown[48], and induce a similar, but not identical, conformational shift in A1492 and A1493 (not shown). Nucleotides G1405 and A1408, methylation of which confers aminoglycoside resistance, are indicated. *Escherichia coli* rRNA nucleotide numbering is used throughout.

the 16S rRNA, including rotation (from 'syn' to 'anti') of the nucleotide G530 base, which in turn provides additional hydrogen-bond support for the flipped-out conformation of A1492 and A1493.

These conformational changes in the 16S rRNA initiate more extensive rearrangements that involve several r-proteins, and result in the movement of the head of the small subunit towards the large subunit[67]. Information from the decoding site is also transmitted directly through the tRNA to the large ribosomal subunit[68,69]. The large subunit and elongation factor Tu respond in concert to this set of signals by triggering hydrolysis of the GTP molecule. The amino acid at the 3′ end of the A-site tRNA is then accommodated into the peptidyl-transferase centre and becomes optimally aligned for addition to the peptide chain (BOX 1). By contrast, no peptide bond will be formed when an A-site tRNA has a mismatched codon–anticodon pair. The irregular backbone of a tRNA–mRNA mismatch will offer insufficient interaction potential for A1492 and A1493 to flip out unaided from helix 44, and therefore no signal for peptide-bond formation will be initiated.

Geneticin and paromomycin are two classes of aminoglycoside drugs that bind within helix 44 adjacent to nucleotides A1492 and A1493 (REFS 47,48,70). Both aminoglycosides are based on a common neamine structure consisting of two amino-sugar rings (I and II), although they differ in the manner in which ring II is substituted with additional sugar residues (FIG. 2). Rings I and II make specific interactions within the distorted major groove of helix 44 at the aminoglycoside-binding site[44,45]. On binding, the drugs coerce A1492 and A1493 to flip out[44–46,48] and adopt a conformation similar to the one described above, but without the participation of G530 (REFS 66,67). Because the aminoglycosides switch the conformation of A1492 and A1493 irrespective of whether there is a cognate codon–anticodon match, they greatly increase the risk that erroneous signals will be conveyed to the large subunit and lead to the addition of incorrect amino acids to the nascent peptide chain.

Mutations[71,72] and methylations[73–75] confer resistance to aminoglycosides by altering their contact surfaces within helix 44. For instance, methylation at the N1 position of nucleotide A1408 by the KamA methyltransferase interferes with the placement of ring I into the aminoglycoside-binding site, and results in resistance to neamine[74]. Methylation of the N7 position of G1405 by the Grm methyltransferase confers resistance to geneticin-class aminoglycosides, but not to paromomycin[73]. This difference between geneticin and paromomycin is due to the relative positions of their ring II substituents, which only in geneticin clash with the methyl group on G1405 (FIG. 3).

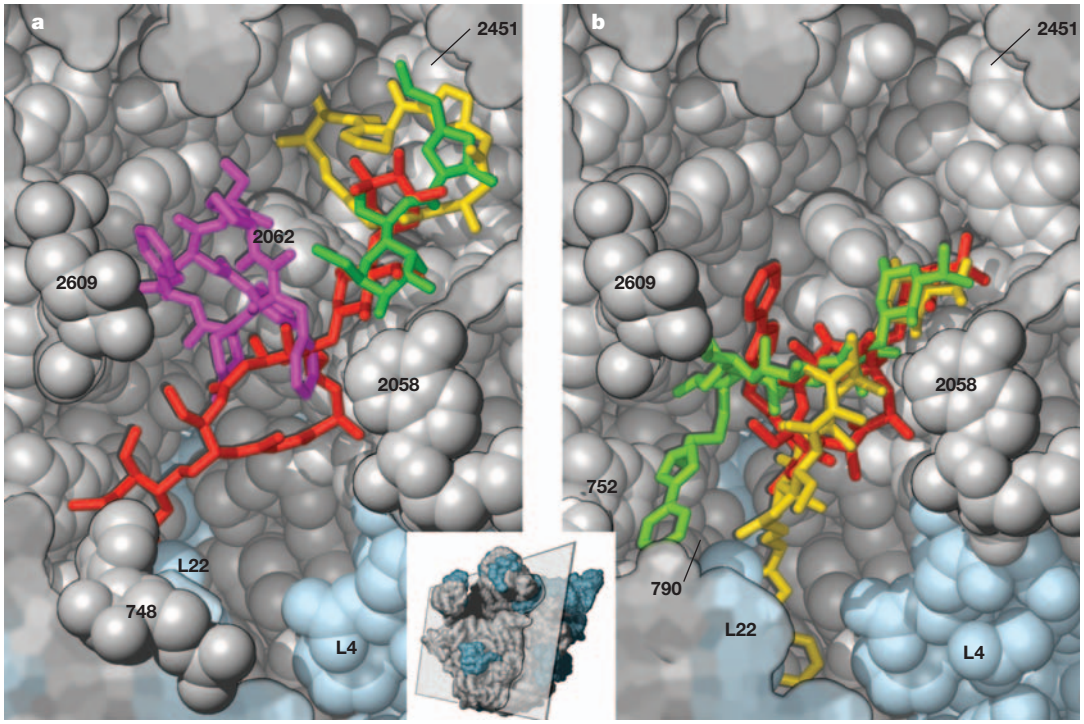

Figure 4 | **Binding sites of macrolide, lincosamide, streptogramin B (MLS_B) antibiotics within the 50S subunit tunnel.** **a** | Subunit cross-section showing the upper portion of the tunnel from the peptidyl-transferase centre (at A2451) to the narrow bend at r-protein L22. The subunit structure is drawn from the coordinates of Tu *et al.*[42]; r-proteins are in blue and rRNA is in grey. The relative positions of the binding sites for the macrolide tylosin (red)[58], the streptogramin A compound dalfopristin (yellow), the streptogramin B compound quinupristin (magenta) and the lincosamide clindamycin (green)[42] are shown. Key nucleotides involved in drug contact and resistance are indicated; some of the nucleotides shown (748, 2058 and 2609) are above the plane of the cross section. Methylation or mutation at nucleotide A2058 disrupts contact and confers resistance to all MLS_B compounds, whereas methylation at G748 affects only tylosin[96]. **b** | The same tunnel section showing the conformations of telithromycin seen in *Haloarcula* 2058A-subunits (red)[42] and in *Deinococcus* subunits (yellow)[102]. The structure in green is a model of telithromycin binding derived from chemical protection on *Escherichia coli* ribosomes[118].

The ribosomal tunnel in the 50S subunit

The newly synthesized peptide chain passes through the 50S subunit tunnel (BOX 1), which is approximately 100 Å in length and runs from the peptidyl-transferase centre at the interface cavity for the P-site tRNA to emerge on the back of the ribosome. The inside wall of the tunnel is highly irregular in shape and in the upper portion closest to the interface it is lined mainly by rRNA (FIG. 4). The narrowest portion of the tunnel is about one-third of the way down, at a bend where the β-HAIRPIN elongations from r-proteins L4 and L22 merge with the rRNA structures. This region of the tunnel has been shown to act as a sensor and control point where the synthesis of certain peptides can be paused (or 'gated'), subject to metabolic requirements[39,41,76]. Perhaps not coincidentally, this is also the region where the MLS_B antibiotics bind (FIG. 4a).

The interaction sites of the MLS_B drugs overlap, and this was first demonstrated by biochemical and genetic studies showing that the drugs bind in a mutually exclusive manner[1,2] and that ribosomes resistant to one MLS_B drug were usually co-resistant to the others[77]. The crystal structures of the MLS_B drugs on the 50S subunit set these earlier data wonderfully in perspective. Superposition of the drugs in the tunnel shows that the structures clearly overlap and make several common contacts around 23S rRNA nucleotide A2058 (FIG. 4a). Nucleotide A2058 has for a long time been recognized as the key player in MLS_B interaction and resistance[78], and the crystal data reveal that each class of drugs forms its own unique set of interactions with additional nucleotides. For instance, streptogramin A and B compounds bind synergistically to adjacent sites[42,60], and in one of the structures, the synergy is suggested to be mediated by a conformational shift in nucleotide A2062 (REF. 42) (FIG. 4a). Lincosamides are smaller molecules and occupy the region between A2058 and the peptidyl-transferase centre, overlapping with the streptogramin A site[42,57]. The macrolides also interact at A2058 but reach further down the tunnel, making contact outside the lincosamide and streptogramin sites.

The site of macrolide antibiotic interaction

Macrolides are naturally occurring POLYKETIDE compounds that are synthesized by actinomycete bacteria. Effective antimicrobials consist of a MACROLACTONE RING of between 14 atoms (in the case of erythromycin) and 16 atoms (tylosin, spiramycin and carbomycin) with many substituents, including up to three neutral and

HAIRPIN
A structural element that makes a 180° turn and doubles back on itself; in proteins, normally formed from a β-strand.

POLYKETIDES
Secondary metabolites that are biosynthesized in a stepwise manner from simple 2-, 3- and 4-carbon building blocks; can have antimicrobial, antifungal, antiparasitic, antitumour or agrochemical properties.

MACROLACTONE RING
The cyclic ester ring at the core of macrolide antibiotics.

amino sugars[79,80]. The sugars make up the main specific contacts with the tunnel wall. Macrolides assert their inhibitory effects by aborting the growth of the nascent peptide chain. Bulky macrolides tend to block peptides as short as two amino acids in length, whereas smaller macrolides allow the chain to reach six to eight residues[81]. Also, the sequence of the peptide can influence its encounter with the drug[82,83]. Furthermore, the 5-disaccharide on the larger macrolides such as tylosin (FIG. 2) reaches back up the tunnel to the peptidyl-transferase centre (FIG. 4a) and directly interferes with peptide-bond formation[1,2,84]. Macrolides have yet another inhibitory effect in their repertoire and block the manufacture of new 50S ribosomal subunits by binding to precursor particles as they are assembled from their r-protein and rRNA components[85].

The structures of naturally occurring macrolides have been manipulated in countless ways to obtain compounds with improved pharmacological properties[79,80,86]. Most new macrolide compounds are semi-synthetic derivatives of erythromycin (FIG. 2) and include azithromycin with its 15-membered ring[80], and the latest generation of derivatives, the ketolides. Telithromycin is the first clinically prescribed ketolide and has shown improved activity against Gram-positive pathogens, including macrolide-resistant strains[87,88]. Macrolide structures have also been altered by genetic manipulation of the polyketide-synthesis operons in the actinomycete producers[86], and this approach holds considerable promise for the production of new compounds with novel pharmacological properties.

Macrolide crystal structures

Crystallographic data on the binding of macrolides to their ribosomal site are presently available for the *Haloarcula* and *Deinococcus* 50S subunits (TABLE 3). Each system has its own strengths: the data from the archaeon *Haloarcula* are better resolved, whereas the bacterial *Deinococcus* system is more closely related to the ribosomes of pathogens. Despite the phylogenetic distinction, the consistency between the two species of ribosome is remarkably good. Both systems show that macrolides bind to the same position of the ribosomal tunnel, with the MACROLIDE 5-AMINO SUGAR, which is essential for drug activity, oriented to form ELECTROSTATIC INTERACTIONS with the polar groups on the 23S rRNA nucleotides 2058 and 2059 (REFS 42,57,58,89) (FIG. 4).

In the *Deinococcus* structure, the 4,5,6-positions of the macrolactone ring fit snugly against the tunnel wall, forming HYDROPHOBIC INTERACTIONS with the minor groove edges of nucleotides A2058 and A2059 (REF. 57). A corresponding fit is hindered in the wild-type *Haloarcula* subunits, in which nucleotide 2058 is a guanosine and has a polar amino group on the minor groove edge that displaces the macrolactone ring towards the lumen of the tunnel[58]. In wild-type bacteria, nucleotide 2058 is an adenosine, and substitution of guanosine causes a 10^4-fold drop in the binding affinity of the macrolide erythromycin[90]. Consistent with this, *Haloarcula* is naturally resistant to macrolides. Binding to wild-type *Haloarcula* subunits was achieved by the use of drug concentrations that were several orders of magnitude above physiological levels[58]. Despite the use of these high drug concentrations (that were comparably high in some of the earlier *Deinococcus* studies[57]), the crystal structures generally fit well with biochemical and genetic data. It is, however, a welcome refinement that G2058 in the *Haloarcula* 23S rRNA has recently been substituted for an adenosine (2058A-subunits)[42], a change which gratifyingly increases the macrolide-binding affinity by 10^4-fold. Intriguingly, this improvement in binding is not accompanied by a change in either the orientation or the conformation of the drugs within the MLS_B site. In the case of azithromycin, binding data are available for wild-type *Haloarcula* subunits[58] and also for 2058A-subunits[42]. The only structural difference seems to be that, in the latter case, azithromycin is shifted about 1 Å closer to A2058 on the tunnel wall.

Some differences in the findings from the *Deinococcus* and *Haloarcula* crystallographic systems remain to be resolved. The conformations of the macrolactone rings are different in the two systems, and forceful cases have been made for the validity of each structure. Salinity differences between *Haloarcula* and bacterial ribosomes could conceivably cause an alternative macrolactone conformation[91], as could sequence differences including 23S rRNA nucleotide 2058 and the neighbouring base pair 2057–2611 (REFS 91,92). These arguments are partly deflected by the recent structures of *Haloarcula* ribosomal subunits with A2058, in which macrolides are bound as tightly as to bacterial subunits[42]. Furthermore, the macrolactone conformation seen in *Haloarcula* ribosomes matches that from an independent NMR study[93], showing that this drug conformation has the lowest free energy in aqueous solution, and would therefore be expected to be more probable from thermodynamic considerations. Whether this reasoning can be extrapolated to the interior of the ribosome where, as discussed above, ribosomal components can take on conformations that would be thermodynamically unfavourable in free solution, is still a matter of contention.

While these differences in the antibiotic conformations are subtle, they are far from trivial, as they influence our perception of drug-binding and resistance mechanisms. We consider two cases below: that of tylosin, in which the crystallographic data match well with the biochemical and genetic data; and that of telithromycin, in which, despite overall agreement on the binding site, the *Deinococcus* and *Haloarcula* crystals and the biochemical and genetic data all point towards different drug conformations.

Tylosin and telithromycin. Tylosin has a 16-membered macrolactone ring with a disaccharide (mycaminose–mycarose) on the 5-position and a mycinose sugar extending from the 14-position (FIG. 2). The crystal structure of wild-type *Haloarcula* 50S subunits[58] shows how the mycaminose amino sugar interacts

MACROLIDE 5-AMINO SUGAR
The nitrogen-containing sugar directly attached to the 5-carbon of the macrolactone ring (desosamine in erythromycin and mycaminose in tylosin).

ELECTROSTATIC INTERACTIONS
Interactions between charged molecules or atoms.

HYDROPHOBIC INTERACTIONS
Interactions that rely on the tendency of non-polar groups to aggregate to avoid contact with a polar solvent.

Table 3 | **Antibiotics that target the 50S ribosomal subunit**

Drug	PDB	Resolution (Å)	System	Ref.
Macrolides and ketolides*				
Carbomycin	1K8A	3.0	*Haloarcula*	58
Spiramycin	1KD1	3.0	*Haloarcula*	58
Tylosin	1K9M	3.0	*Haloarcula*	58
Azithromycin	1M1K	3.2	*Haloarcula*	58
Azithromycin	1NWY	3.3	*Deinococcus*	89
Azithromycin	1YHQ	2.4	*Haloarc-2058A*	42
Erythromycin	1JZY	3.5	*Deinococcus*	57
Erythromycin	1YI2	2.7	*Haloarc-2058A*	42
Clarithromycin	1J5A	3.5	*Deinococcus*	57
Roxithromycin	1JZZ	3.8	*Deinococcus*	57
Troleandomycin	1OND	3.4	*Deinococcus*	40
ABT 773	1NWX	3.5	*Deinococcus*	89
Telithromycin	1P9X	3.4	*Deinococcus*	102
Telithromycin	1YIJ	2.6	*Haloarc-2058A*	42
Streptogramin A‡				
Virginiamycin M	1N8R	3.0	*Haloarcula*	59
Virginiamycin M	1YIT	2.8	*Haloarc-2058A*	42
Dalfopristin	1SM1	3.4	*Deinococcus*	60
Streptogramin B§				
Quinupristin	1SM1	3.4	*Deinococcus*	60
Quinupristin	1YJW	2.9	*Haloarc-2058A*	42
Lincosamides‡				
Clindamycin	1JZX	3.1	*Deinococcus*	57
Clindamycin	1YJN	3.0	*Haloarc-2058A*	42
Nucleoside based‖				
Chloramphenicol	1K01	3.5	*Deinococcus*	57
Chloramphenicol	1NJI	3.0	*Haloarcula*	59
Anisomycin	1K73	3.0	*Haloarcula*	59
Sparsomycin	1M90	2.8	*Haloarcula*	59
Blasticidin S	1KC8	3.0	*Haloarcula*	59
Puromycin derivative	1FFZ	3.2	*Haloarcula*	16
Pleuromutilins‡				
Tiamulin	1XBP	3.5	*Deinococcus*	62
Valnemulin	–	–	nd	–
Oxazolidinones¶				
Linezolid	–	–	np	–
XA043	–	–	nd	–

*Bind in peptide exit tunnel and interfere with the elongation of the nascent peptide. Some 16-membered macrolides (tylosin, carbomycin and spiramycin) also inhibit peptide-bond formation. ‡Block peptide-bond formation. §Prevent elongation of nascent peptide. ‖Various effects. ¶Decrease translational fidelity. Thiopeptide compounds, such as thiostrepton and micrococcin, interfere with guanosine-nucleotide-triphosphate hydrolysis, whereas orthosomycins, such as avilamycin and evernimycin, interfere with binding of transfer RNA and possibly initiation factor-2. Crystal structures have not been determined for these antibiotics. The *Deinococcus* and *Haloarcula* systems refer to 50S subunits from the bacterium *Deinococcus radiodurans* and the archaeon *Haloarcula marismortui*, respectively; *Haloarc-2058A* are *Haloarcula* 50S subunits containing a G2058 to A2058 substitution in the 23S rRNA. nd, crystal structure not determined; np, not published; PDB, Protein Data Bank ID.

with nucleotide 2058, while the mycarose extends further up the tunnel towards the peptidyl-transferase centre. The mycinose sugar attaches the drug to the opposite side of the tunnel by contacting the rRNA at nucleotide 748 (FIG. 4a). This orientation of tylosin in its binding site fits with the chemical-protection data[84], and is also consistent with the genetic data on tylosin resistance[94–97] (discussed below).

Telithromycin binds more strongly to ribosomes than the parent macrolide erythromycin, largely because of the alkyl-aryl substituent extending from the macrolactone-ring positions 11 and 12 (REFS 98,99) (FIG. 2). In *Haloarcula* 2058A-subunits, the aryl moiety contributes to telithromycin's binding by stacking onto the base of nucleotide 2609 (FIG. 4b). This fits well with some of the data from chemical-protection and genetic studies on *E. coli* ribosomes[100,101], but less well with other data showing protection at nucleotide A752 (REFS 98,99). In *Deinococcus* 50S crystals[102], telithromycin binds to the same region of the tunnel, but its macrolactone ring has a stretched conformation compared with the structure in *Haloarcula* 50S, and this orients the alkyl-aryl substituent further down the tunnel (FIG. 4b).

So far, the reasons for these discrepancies are not clear. Biochemical and genetic data have repeatedly proven their worth in identifying drug-binding sites, but extrapolating these data to form structural models is fraught with difficulty. Crystallography is by far the most accurate structural approach, although comparison of data is complicated by differences in the systems discussed above. On the basis of available data, it is feasible that the conformation of telithromycin might be different when bound to ribosomes from *Escherichia*, *Deinococcus* and *Haloarcula*.

Resistance to macrolides

Mutations at nucleotide 2058 and its neighbours alter the main anchoring point for macrolides and tend to confer strong resistance to most of these drugs[103], presumably by disturbing the drug fit in its binding site[28,42,91,104]. More modest resistance effects limited to certain macrolide subgroups are brought about by mutations around nucleotide 752 (REFS 97,98) and by mutations in r-proteins L4 and L22 (REFS 105–109). The r-protein mutations are invariably at the ends of the L4 and L22 hairpin structures situated close to the MLS_B site, and can be seen from cryo-electron microscopy[38] and biochemical studies[110] to affect the tunnel shape and rRNA accessibility. The L22 mutations confer resistance without reducing binding affinity for erythromycin[105,106], and this is explained by a local change in the L22 hairpin[111] that increases the tunnel width at the MLS_B site to allow passage of the nascent peptide despite erythromycin binding[42].

In many pathogenic and macrolide-producing bacteria, resistance is caused by methylation of the rRNA[75] rather than by mutation. Specific methylation of the N6 position of nucleotide A2058 in the 23S rRNA is catalysed by members of the Erm family of methyltransferases[112]. Erm methyltransferases differ according

to whether they add one or two methyl groups to this nucleotide position[77,113]. Monomethylation confers the so-called MLS_B type I phenotype, with high resistance to lincosamides, low-to-moderate resistance to macrolide and streptogramin B antibiotics[77,94], but no resistance to ketolides such as telithromycin[114]. Erm dimethyltransferases confer the MLS_B type II phenotype, with high resistance to all MLS_B antibiotics[77,115] and to telithromycin[114], and this is the more common resistance mechanism in bacterial pathogens.

Dimethylation at the N6 of A2058 occludes the main contact site for all the MLS_B drugs and constitutes the most effective form of resistance against these drugs. It is surprising therefore that, in addition to an Erm dimethyltransferase, some bacteria have their own idiosyncratic resistance mechanisms. For instance, the tylosin-producing actinomycete *Streptomyces fradiae* has a combination of Erm mono- and dimethyltransferases[94,95] in addition to a third methyltransferase ($RlmA^{II}$) that is specific for the N1 of nucleotide G748 (REF. 116). The Erm dimethyltransferase is first expressed when tylosin levels are relatively high. Up to this point, tylosin resistance is conferred by the synergistic action of the Erm monomethyltransferase and $RlmA^{II}$, with neither methylation on its own causing any appreciable reduction in tylosin binding[96]. The N1 of G748 points into the lumen of the 50S ribosomal-subunit tunnel facing nucleotide A2058 approximately 15 Å away[31,32], and the resistance mechanism is explained by the position of tylosin in its binding site[58] (FIG. 4a). It is not clear why *S. fradiae* has retained this array of rRNA methyltransferases, and the methylations could possibly have other functions, such as facilitating the passage of the nascent peptide through the tunnel.

Where to from here?

The high-resolution crystal structures of the antibiotic-binding sites make interpretation of much of the biochemical and genetic data more or less straightforward. From the crystal structures, we can now perceive how drugs exercise their inhibitory effects, how drugs with overlapping sites can mutually exclude each other's binding, as well as how mutations and methylations confer resistance to specific or multiple drug classes. Also, the crystal structures help us to speculate about how existing drugs might be improved, or novel drugs created, to circumvent resistance.

Derivatizing existing drugs to improve interaction at their binding site is an approach that has received considerable attention in the pharmaceutical industry, and is illustrated by the macrolide drugs[79,80,86] and the most recent ketolide derivatives[101,117]. Rational approaches based on crystallographic data have been applied to the design of new aminoglycosides[49] and to the development of hybrid drugs, such as chimaeric oxazolidinone–macrolide compounds based on linezolid and azithromycin[123]. Presumably, these novel drugs target the same sites as the parent compounds, but do so with greater affinity.

A considerably greater challenge is how to identify and target unexploited sites with novel drugs. A large variety of natural compounds inhibit the ribosome by binding to relatively few sites (FIG. 1). So far, we do not know whether these are the only sites that are effective points of inhibition, or whether there are other possible sites that remain undiscovered — either owing to our lack of observational skill or because three and a half billion years of evolution has been too short a time to try them out. The ribosomal tunnel offers a plethora of nooks and crannies that could potentially act as target sites. For instance, a putative second azithromycin site further down the tunnel[89], although as yet uncorroborated, could indicate a potential site against which to design a novel drug.

In conclusion, we find ourselves in an exciting new era of ribosome and antibiotic research, although the work cited here is by no means the final chapter concerning what we need to know about the ribosome. The ribosome is a complex, dynamic machine that directs the multi-stage process of translation. Snapshots of several of these stages have been captured by cryo-electron microscopy, whereas fewer, but more highly resolved, shots have been caught by crystallography. Although these still-frame pictures are impressive and informative, we are still looking forward to seeing the entire 'movie' of protein synthesis at high resolution. The present crystal structures form a basis for understanding and improving antimicrobials and, together with additional and better-resolved data, will undoubtedly lead to the rational design of effective novel compounds.

1. Vázquez, D. *Inhibitors of Protein Biosynthesis* (Springer–Verlag, Berlin, 1979).
2. Gale, E. F., Cundliffe, E., Reynolds, P. E., Richmond, M. H. & Waring, M. J. *The Molecular Basis of Antibiotic Action* (John Wiley and Sons, London, 1981).
3. Spahn, C. M. & Prescott, C. D. Throwing a spanner in the works: antibiotics and the translation apparatus. *J. Mol. Med.* **74**, 423–439 (1996).
4. Mankin, A. S. Ribosomal antibiotics. *Mol. Biol.* **35**, 509–520 (2001).
5. Lake, J. A. Ribosome structure determined by electron microscopy of *Escherichia coli* small subunits, large subunits and monomeric ribosomes. *J. Mol. Biol.* **105**, 131–139 (1976).
6. Tischendorf, G. W., Zeichhardt, H. & Stoffler, G. Architecture of the *Escherichia coli* ribosome as determined by immune electron microscopy. *Proc. Natl Acad. Sci. USA* **72**, 4820–4824 (1975).
7. Boublik, M., Hellmann, W. & Kleinschmidt, A. K. Size and structure of *Escherichia coli* ribosomes by electron microscopy. *Cytobiologie* **14**, 293–300 (1977).
8. Pape, T., Stark, H., Matadeen, R., Orlova, E. V. & van Heel, M. in *The Ribosome: Structure, Function, Antibiotics and Cellular Interactions* (eds Garrett, R. A. *et al.*) 37–44 (American Society for Microbiology, Washington DC, 2000).
9. Agrawal, R. K. & Frank, J. Structural studies of the translational apparatus. *Curr. Opin. Struct. Biol.* **9**, 215–221 (1999).
10. Frank, J. *et al.* The role of tRNA as a molecular spring in decoding, accommodation, and peptidyl transfer. *FEBS Lett.* **579**, 959–962 (2005).
11. Valle, M. *et al.* Visualizing tmRNA entry into a stalled ribosome. *Science* **300**, 127–130 (2003).
12. Valle, M. *et al.* Incorporation of aminoacyl-tRNA into the ribosome as seen by cryo-electron microscopy. *Nature Struct. Biol.* **10**, 899–906 (2003).

References 11 and 12 illustrate the power of the cryo-EM technique for viewing the ribosome at isolated steps in the translation process.

13. Noller, H. F., Hoffarth, V. & Zimniak, L. Unusual resistance of peptidyl transferase to protein extraction procedures. **256**, 1416–1419 (1992).
14. Green, R., Switzer, C. & Noller, H. F. Ribosome-catalyzed peptide-bond formation with an A-site substrate covalently linked to 23S ribosomal RNA. *Science* **280**, 286–289 (1998).
15. Zhang, B. & Cech, T. R. Peptide bond formation by *in vitro* selected ribozymes. *Nature* **390**, 96–100 (1997).
16. Nissen, P., Hansen, J., Ban, N., Moore, P. B. & Steitz, T. A. The structural basis of ribosome activity in peptide bond synthesis. *Science* **289**, 920–930 (2000).

The first structural data strongly indicating that peptide-bond formation is RNA-catalysed, and implicating 23S rRNA nucleotide A2451 in this process.

17. Bashan, A. *et al.* Structural basis of the ribosomal machinery for peptide bond formation, translocation, and nascent chain progression. *Mol. Cell* **11**, 91–102 (2003).
18. Moore, P. B. & Steitz, T. A. The structural basis of large ribosomal subunit function. *Annu. Rev. Biochem.* **72**, 813–850 (2003).
19. Sievers, A., Beringer, M., Rodnina, M. V. & Wolfenden, R. The ribosome as an entropy trap. *Proc. Natl Acad. Sci. USA* **101**, 7897–7901 (2004).
20. Youngman, E. M., Brunelle, J. L., Kochaniak, A. B. & Green, R. The active site of the ribosome is composed of two layers of conserved nucleotides with distinct roles in peptide bond formation and peptide release. *Cell* **117**, 589–599 (2004).
21. Erlacher, M. D. *et al.* Chemical engineering of the peptidyl transferase center reveals an important role of the 2′-hydroxyl group of A2451. *Nucleic Acids Res.* **33**, 1618–1627 (2005).
A cleverly designed biochemical/molecular genetic study of peptide-bond formation and the role of the nucleotide A2451 ribose. This article's introduction concisely sums up previous research and discussions on this topic.
22. Yonath, A., Mussig, J. & Wittmann, H. G. Parameters for crystal growth of ribosomal subunits. *J. Cell. Biochem.* **19**, 145–155 (1982).
23. Trakhanov, S. *et al.* Preliminary X-ray investigation of 70 S ribosome crystals from *Thermus thermophilus*. *J. Mol. Biol.* **209**, 327–328 (1989).
24. von Bohlen, K. *et al.* Characterization and preliminary attempts for derivatization of crystals of large ribosomal subunits from *Haloarcula marismortui* diffracting to 3 Å resolution. *J. Mol. Biol.* **222**, 11–15 (1991).
25. Yusupov, M. M., Garber, M. B., Vasiliev, V. D. & Spirin, A. S. *Thermus thermophilus* ribosomes for crystallographic studies. *Biochimie* **73**, 887–897 (1991).
26. Liljas, A. *Structural aspects of protein synthesis* (World Scientific, Singapore, 2004).
27. Wimberly, B. T. *et al.* Structure of the 30S ribosomal subunit. *Nature* **407**, 327–339 (2000).
28. Schluenzen, F. *et al.* Structure of functionally activated small ribosomal subunit at 3.3 Å resolution. *Cell* **102**, 615–623 (2000).
29. Yusupov, M. M. *et al.* Crystal structure of the ribosome at 5.5 Å resolution. *Science* **292**, 883–896 (2001).
Describes the crystal structures of both ribosomal subunits in functional complexes, and reveals essential details of tRNA interactions and how the ribosome works.
30. Yusupova, G. Z., Yusupov, M. M., Cate, J. H. & Noller, H. F. The path of messenger RNA through the ribosome. *Cell* **106**, 233–241 (2001).
31. Ban, N., Nissen, P., Hansen, J., Moore, P. B. & Steitz, T. A. The complete atomic structure of the large ribosomal subunit at 2.4 Å resolution. *Science* **289**, 905–920 (2000).
32. Harms, J. *et al.* High resolution structure of the large ribosomal subunit from a mesophilic eubacterium. *Cell* **107**, 679–688 (2001).
33. Vila-Sanjurjo, A. *et al.* X-ray crystal structures of the WT and a hyper-accurate ribosome from *Escherichia coli*. *Proc. Natl Acad. Sci. USA* **100**, 8682–8687 (2003).
First structure of *E. coli* ribosomes, which had previously been thought to be refractory to crystallographic analysis. Presently at low resolution, but more highly resolved data are on the way.
34. Klein, D. J., Moore, P. B. & Steitz, T. A. The roles of ribosomal proteins in the structure assembly, and evolution of the large ribosomal subunit. *J. Mol. Biol.* **340**, 141–177 (2004).
35. Semrad, K., Green, R. & Schroeder, R. RNA chaperone activity of large ribosomal subunit proteins from *Escherichia coli*. *RNA* **10**, 1855–1860 (2004).
36. Noller, H. F. The driving force for molecular evolution of translation. *RNA* **10**, 1833–1837 (2004).
37. Takyar, S., Hickerson, R. P. & Noller, H. F. mRNA helicase activity of the ribosome. *Cell* **120**, 49–58 (2005).
38. Gabashvili, I. S. *et al.* The polypeptide tunnel system in the ribosome and its gating in erythromycin resistance mutants of L4 and L22. *Mol. Cell* **8**, 181–188 (2001).
39. Tenson, T. & Ehrenberg, M. Regulatory nascent peptides in the ribosomal tunnel. *Cell* **108**, 591–594 (2002).
40. Berisio, R. *et al.* Structural insight into the role of the ribosomal tunnel in cellular regulation. *Nature Struct. Biol.* **10**, 366–370 (2003).
41. Nakatogawa, H., Murakami, A. & Ito, K. Control of SecA and SecM translation by protein secretion. *Curr. Opin. Microbiol.* **7**, 145–150 (2004).
42. Tu, D., Blaha, G., Moore, P. B. & Steitz, T. A. Structures of MLS_BK antibiotics bound to mutated large ribosomal subunits provide a structural explanation for resistance. *Cell* **121**, 257–270 (2005).
An important refinement in the use of *Haloarcula* subunits for antibiotic binding studies. Also sheds light on the mechanisms of nucleotide A2058 and r-protein L22 mutations in macrolide resistance.
43. Ferbitz, L. *et al.* Trigger factor in complex with the ribosome forms a molecular cradle for nascent proteins. *Nature* **431**, 590–596 (2004).
44. Fourmy, D., Recht, M. I., Blanchard, S. C. & Puglisi, J. D. Structure of the A site of *Escherichia coli* 16S ribosomal RNA complexed with an aminoglycoside antibiotic. *Science* **274**, 1367–1371 (1996).
45. Yoshizawa, S., Fourmy, D. & Puglisi, J. D. Structural origins of gentamicin antibiotic action. *EMBO J.* **17**, 6437–6448 (1998).
46. Carter, A. P. *et al.* Functional insights from the structure of the 30S ribosomal subunit and its interactions with antibiotics. *Nature* **407**, 340–348 (2000).
References 16, 46 and 57 are examples of initial ground-breaking studies by three different research groups that revealed the molecular details of ribosomal subunits and antibiotic interactions. For all these studies, the readers are referred to the atomic coordinates in the databases (Tables 2 and 3).
47. Vicens, Q. & Westhof, E. Crystal structure of paromomycin docked into the eubacterial ribosomal decoding A site. *Structure (Camb.)* **9**, 647–658 (2001).
48. Vicens, Q. & Westhof, E. Crystal structure of geneticin bound to a bacterial 16S ribosomal RNA A site oligonucleotide. *J. Mol. Biol.* **326**, 1175–1188 (2003).
49. Hermann, T. Drugs targeting the ribosome. *Curr. Opin. Struct. Biol.* **15**, 355–366 (2005).
50. Rodnina, M. V. *et al.* Thiostrepton inhibits the turnover but not the GTPase of elongation factor G on the ribosome. *Proc. Natl Acad. Sci. USA* **96**, 9586–9590 (1999).
51. Brandi, L. *et al.* The translation initiation functions of IF2: targets for thiostrepton inhibition. *J. Mol. Biol.* **335**, 881–894 (2004).
52. Bowen, W. S., Van Dyke, N., Murgola, E. J., Lodmell, J. S. & Hill, W. E. Interaction of thiostrepton and elongation factor-G with the ribosomal protein L11-binding domain. *J. Biol. Chem.* **280**, 2934–2943 (2005).
53. McNicholas, P. M. *et al.* Evernimicin binds exclusively to the 50S ribosomal subunit and inhibits translation in cell-free systems derived from both Gram-positive and Gram-negative bacteria. *Antimicrob. Agents Chemother.* **44**, 1121–1126 (2000).
54. Belova, L., Tenson, T., Xiong, L., McNicholas, P. M. & Mankin, A. S. A novel site of antibiotic action in the ribosome: interaction of evernimicin with the large ribosomal subunit. *Proc. Natl Acad. Sci. USA* **98**, 3726–3731 (2001).
55. Kofoed, C. B. & Vester, B. Interaction of avilamycin with ribosomes and resistance caused by mutations in 23S rRNA. *Antimicrob. Agents Chemother.* **46**, 3339–3342 (2002).
56. Treede, I. *et al.* The avilamycin resistance determinants AviRa and AviRb methylate 23S rRNA at the guanosine 2535 base and the uridine 2479 ribose. *Mol. Microbiol.* **49**, 309–318 (2003).
57. Schlunzen, F. *et al.* Structural basis for the interaction of antibiotics with the peptidyl transferase centre in eubacteria. *Nature* **413**, 814–821 (2001).
58. Hansen, J. L. *et al.* The structures of four macrolide antibiotics bound to the large ribosomal subunit. *Mol. Cell* **10**, 117–128 (2002).
59. Hansen, J. L., Moore, P. B. & Steitz, T. A. Structures of five antibiotics bound at the peptidyl transferase center of the large ribosomal subunit. *J. Mol. Biol.* **330**, 1061–1075 (2003).
60. Harms, J. M., Schlunzen, F., Fucini, P., Bartels, H. & Yonath, A. Alterations at the peptidyl transferase centre of the ribosome induced by the synergistic action of the streptogramins dalfopristin and quinupristin. *BMC Biol.* **2**, 4 (2004).
61. Pringle, M., Poehlsgaard, J., Vester, B. & Long, K. S. Mutations in ribosomal protein L3 and 23S ribosomal RNA at the peptidyl transferase centre are associated with reduced susceptibility to tiamulin in *Brachyspira* spp. isolates. *Mol. Microbiol.* **54**, 1295–1306 (2004).
62. Schlunzen, F., Pyetan, E., Fucini, P., Yonath, A. & Harms, J. M. Inhibition of peptide bond formation by pleuromutilins: the structure of the 50S ribosomal subunit from *Deinococcus radiodurans* in complex with tiamulin. *Mol. Microbiol.* **54**, 1287–1294 (2004).
63. Kloss, P., Xiong, L., Shinabarger, D. L. & Mankin, A. S. Resistance mutations in 23 S rRNA identify the site of action of the protein synthesis inhibitor linezolid in the ribosomal peptidyl transferase center. *J. Mol. Biol.* **294**, 93–101 (1999).
64. Thompson, J., O'Connor, M., Mills, J. A. & Dahlberg, A. E. The protein synthesis inhibitors, oxazolidinones and chloramphenicol, cause extensive translational inaccuracy *in vivo*. *J. Mol. Biol.* **322**, 273–279 (2002).
65. Yoshizawa, S., Fourmy, D. & Puglisi, J. D. Recognition of the codon-anticodon helix by ribosomal RNA. *Science* **285**, 1722–1725 (1999).
First conclusive experimental data that link the 16S rRNA bases A1492 and A1493 with the decoding process.
66. Ogle, J. M. *et al.* Recognition of cognate transfer RNA by the 30S ribosomal subunit. *Science* **292**, 897–902 (2001).
Crystal study that confirms the involvement of A1492 and A1493 in the decoding process and links their movement with other conformational changes in the 30S ribosomal subunit. See also reference 67 for a review.
67. Ogle, J. M., Carter, A. P. & Ramakrishnan, V. Insights into the decoding mechanism from recent ribosome structures. *Trends Biochem. Sci.* **28**, 259–266 (2003).
68. Piepenburg, O. *et al.* Intact aminoacyl-tRNA is required to trigger GTP hydrolysis by elongation factor Tu on the ribosome. *Biochemistry* **39**, 1734–1738 (2000).
69. Cochella, L. & Green, R. An active role for tRNA in decoding beyond codon:anticodon pairing. *Science* **308**, 1178–1180 (2005).
70. Moazed, D. & Noller, H. F. Interaction of antibiotics with functional sites in 16S ribosomal RNA. *Nature* **327**, 389–394 (1987).
71. Pfister, P. *et al.* Mutagenesis of 16S rRNA C1409–G1491 base-pair differentiates between 6′-OH and 6′-NH^{3+} aminoglycosides. *J. Mol. Biol.* **346**, 467–475 (2005).
72. Gregory, S. T., Carr, J. F. & Dahlberg, A. E. A mutation in the decoding center of *Thermus thermophilus* 16S rRNA suggests a novel mechanism of streptomycin resistance. *J. Bacteriol.* **187**, 2200–2202 (2005).
73. Thompson, J., Skeggs, P. A. & Cundliffe, E. Methylation of 16S ribosomal RNA and resistance to the aminoglycoside antibiotics gentamicin and kanamycin determined by DNA from the gentamicin-producer, *Micromonospora purpurea*. *Mol. Gen. Genet.* **201**, 168–173 (1985).
74. Beauclerk, A. A. & Cundliffe, E. Sites of action of two ribosomal RNA methylases responsible for resistance to aminoglycosides. *J. Mol. Biol.* **193**, 661–671 (1987).
75. Douthwaite, S., Fourmy, D. & Yoshizawa, S. in *Fine-tuning of RNA Functions by Modification and Editing* (ed. Grosjean, H.) 287–309 (Springer–Verlag, New York, 2005).
76. Gong, F. & Yanofsky, C. Instruction of translating ribosome by nascent peptide. *Science* **297**, 1864–1867 (2002).
77. Weisblum, B. Erythromycin resistance by ribosome modification. *Antimicrob. Agents Chemother.* **39**, 577–585 (1995).
78. Cundliffe, E. in *The Ribosome: Structure, Function and Evolution* (eds Hill, W. E. *et al.*) 479–490 (American Society for Microbiology, Washington DC, 1990).
79. Bryskier, A. J., Butzler, J. P., Neu, H. C. & Tulkens, P. M. *Macrolides: Chemistry, Pharmacology and Clinical Uses* (Arnette Blackwell, Paris, 1993).
80. Schönfeld, W. & Kirst, H. A. (eds) *Macrolide Antibiotics* (Birkhäuser, Basel, 2002).
81. Tenson, T., Lovmar, M. & Ehrenberg, M. The mechanism of action of macrolides, lincosamides and streptogramin B reveals the nascent peptide exit path in the ribosome. *J. Mol. Biol.* **330**, 1005–1014 (2003).
82. Weisblum, B. Insights into erythromycin action from studies of its activity as inducer of resistance. *Antimicrob. Agents Chemother.* **39**, 797–805 (1995).
83. Tenson, T. & Mankin, A. S. Short peptides conferring resistance to macrolide antibiotics. *Peptides* **22**, 1661–1668 (2001).
84. Poulsen, S. M., Kofoed, C. & Vester, B. Inhibition of the ribosomal peptidyl transferase reaction by the mycarose moiety of the antibiotics carbomycin, spiramycin and tylosin. *J. Mol. Biol.* **304**, 471–481 (2000).
85. Champney, W. S. Bacterial ribosomal subunit assembly is an antibiotic target. *Curr. Top. Med. Chem.* **3**, 929–947 (2003).
86. Katz, L. & Ashley, G. W. Translation and protein synthesis: macrolides. *Chem. Rev.* **105**, 499–528 (2005).
87. Bryskier, A. Ketolides — telithromycin, an example of a new class of antibacterial agents. *Clin. Microbial. Infect.* **6**, 661–669 (2000).
88. Farrell, D. J. & Felmingham, D. Activities of telithromycin against 13,874 *Streptococcus pneumoniae* isolates collected between 1999 and 2003. *Antimicrob. Agents Chemother.* **48**, 1882–1884 (2004).
89. Schlunzen, F. *et al.* Structural basis for the antibiotic activity of ketolides and azalides. *Structure (Camb.)* **11**, 329–338 (2003).

90. Douthwaite, S. & Aagaard, C. Erythromycin binding is reduced in ribosomes with conformational alterations in the 23S rRNA peptidyl transferase loop. **232**, 725–731 (1993).
91. Yonath, A. & Bashan, A. Ribosomal crystallography: initiation, peptide bond formation, and amino acid polymerization are hampered by antibiotics. *Annu. Rev. Microbiol.* **58**, 233–251 (2004).
92. Pfister, P. *et al.* 23S rRNA base pair 2057–2611 determines ketolide susceptibility and fitness cost of the macrolide resistance mutation 2058A to G. *Proc. Natl Acad. Sci. USA* **102**, 5180–5185 (2005).
93. Awan, A., Brennan, R. J., Regan, A. C. & Barber, J. The conformations of the macrolide antibiotics erythromycin A, azithromycin and clarithromycin in aqueous solution: a H-1 NMR study. *J. Chem. Soc. Perkin Trans. I* **2**, 1645–1652 (2000).
94. Zalacain, M. & Cundliffe, E. Cloning of *tlrD*, a fourth resistance gene, from the tylosin producer, *Streptomyces fradiae*. *Gene* **97**, 137–142 (1991).
95. Zalacain, M. & Cundliffe, E. Methylation of 23S rRNA caused by *tlrA* (*ermSF*), a tylosin resistance determinant from *Streptomyces fradiae*. *J. Bacteriol.* **171**, 4254–4260 (1989).
96. Liu, M. & Douthwaite, S. Resistance to the macrolide antibiotic tylosin is conferred by single methylations at 23S rRNA nucleotides G748 and A2058 acting in synergy. *Proc. Natl Acad. Sci. USA* **99**, 14658–14663 (2002).
97. Novotny, G. W., Jakobsen, L., Andersen, N. M., Poehlsgaard, J. & Douthwaite, S. Ketolide antimicrobial activity persists after disruption of interactions with domain II of 23S rRNA. *Antimicrob. Agents Chemother.* **48**, 3677–3683 (2004).
98. Xiong, L., Shah, S., Mauvais, P. & Mankin, A. S. A ketolide resistance mutation in domain II of 23S rRNA reveals the proximity of hairpin 35 to the peptidyl transferase centre. *Mol. Microbiol.* **31**, 633–639 (1999).
99. Hansen, L. H., Mauvais, P. & Douthwaite, S. The macrolide-ketolide antibiotic binding site is formed by structures in domains II and V of 23S ribosomal RNA. *Mol. Microbiol.* **31**, 623–631 (1999).
100. Garza-Ramos, G., Xiong, L., Zhong, P. & Mankin, A. Binding site of macrolide antibiotics on the ribosome: new resistance mutation identifies a specific interaction of ketolides with rRNA. *J. Bacteriol.* **183**, 6898–6907 (2001).
101. Xiong, L., Korkhin, Y. & Mankin, A. S. Binding site of the bridged macrolides in the Escherichia coli ribosome. *Antimicrob. Agents Chemother.* **49**, 281–288 (2005).
102. Berisio, R. *et al.* Structural insight into the antibiotic action of telithromycin against resistant mutants. *J. Bacteriol.* **185**, 4276–4279 (2003).
103. Vester, B. & Douthwaite, S. Macrolide resistance conferred by base substitutions in 23S rRNA. *Antimicrob. Agents Chemother.* **45**, 1–12 (2001).
104. Pfister, P. *et al.* The structural basis of macrolide-ribosome binding assessed using mutagenesis of 23S rRNA positions 2058 and 2059. *J. Mol. Biol.* **342**, 1569–1581 (2004).
105. Wittmann, H. G. *et al.* Biochemical and genetic studies on two different types of erythromycin resistant mutants of *Escherichia coli* with altered ribosomal proteins. *Mol. Gen. Genet.* **127**, 175–189 (1973).
106. Pardo, D. & Rosset, R. Properties of ribosomes from erythromycin resistant mutants of *Escherichia coli*. *Mol. Gen. Genet.* **156**, 267–271 (1977).
107. Chittum, H. S. & Champney, W. S. Ribosomal protein gene sequence changes in erythromycin-resistant mutants of *Escherichia coli*. *J. Bacteriol.* **176**, 6192–6198 (1994).
108. Tait-Kamradt, A. *et al.* Mutations in 23S rRNA and ribosomal protein L4 account for resistance in pneumococcal strains selected *in vitro* by macrolide passage. *Antimicrob. Agents Chemother.* **44**, 2118–2125 (2000).
109. Farrell, D. J., Morrissey, I., Bakker, S., Buckridge, S. & Felmingham, D. *In vitro* activities of telithromycin, linezolid, and quinupristin-dalfopristin against *Streptococcus pneumoniae* with macrolide resistance due to ribosomal mutations. *Antimicrob. Agents Chemother.* **48**, 3169–3171 (2004).
110. Gregory, S. T. & Dahlberg, A. E. Erythromycin resistance mutations in ribosomal proteins L22 and L4 perturb the higher order structure of 23 S ribosomal RNA. *J. Mol. Biol.* **289**, 827–834 (1999).
111. Davydova, N., Streltsov, V., Wilce, M., Liljas, A. & Garber, M. L22 ribosomal protein and effect of its mutation on ribosome resistance to erythromycin. *J. Mol. Biol.* **322**, 635–644 (2002).
112. Skinner, R., Cundliffe, E. & Schmidt, F. J. Site of action of a ribosomal RNA methylase responsible for resistance to erythromycin and other antibiotics. *J. Biol. Chem.* **258**, 12702–12706 (1983).
113. Roberts, M. C. Resistance to macrolide, lincosamide, streptogramin, ketolide, and oxazolidinone antibiotics. *Mol. Biotechnol.* **28**, 47–62 (2004).
114. Liu, M. & Douthwaite, S. Activity of the ketolide telithromycin is refractory to Erm monomethylation of bacterial rRNA. *Antimicrob. Agents Chemother.* **46**, 1629–1633 (2002).
115. Sutcliffe, J. A. & Leclercq, R. in *Macrolide Antibiotics* (eds Schönfeld, W. & Kirst, H. A.) 281–317 (Birkhäuser, Berlin, 2002).
116. Douthwaite, S., Crain, P. F., Liu, M. & Poehlsgaard, J. The tylosin-resistance methyltransferase RlmA^{II} (TlrB) modifies the N-1 position of 23S rRNA nucleotide G748. *J. Mol. Biol.* **337**, 1073–1077 (2004).
117. Abbanat, D. *et al. In vitro* activities of novel 2-fluoro-naphthyridine-containing ketolides. *Antimicrob. Agents Chemother.* **49**, 309–315 (2005).
118. Poehlsgaard, J. & Douthwaite, S. The macrolide binding site on the bacterial ribosome. *Curr. Drug Targets Infect. Disord.* **2**, 67–78 (2002).
119. Brodersen, D. E. *et al.* The structural basis for the action of the antibiotics tetracycline, pactamycin, and hygromycin B on the 30S ribosomal subunit. *Cell* **103**, 1143–1154 (2000).
120. Vicens, Q. & Westhof, E. Crystal structure of a complex between the aminoglycoside tobramycin and an oligonucleotide containing the ribosomal decoding a site. *Chem. Biol.* **9**, 747–755 (2002).
121. Han, Q. *et al.* Molecular recognition by glycoside pseudo base pairs and triples in an apramycin–RNA complex. *Angew. Chem. (Int. Ed. Engl.)* **44**, 2694–2700 (2005).
122. Pioletti, M. *et al.* Crystal structures of complexes of the small ribosomal subunit with tetracycline, edeine and IF3. *EMBO J.* **20**, 1829–1839 (2001).
123. Sutcliffe, J. Rib-X Pharmaceuticals. Antibiotics Conference, Tartu, Estonia, June 2005.

Acknowledgements

Support from the Danish Research Agency and the Nucleic Acid Center of the Danish Grundforskningsfond are gratefully acknowledged.

Competing interests statement

The authors declare no competing financial interests.

Online links

DATABASES

The following terms in this article are linked online to:

Entrez: http://www.ncbi.nlm.nih.gov/Entrez

Deinococcus radiodurans | *Escherichia coli* | *Haloarcula marismortui* | *Thermus thermophilus*

FURTHER INFORMATION

Stephen Douthwaite's laboratory:
http://www.sdu.dk/Nat/bmb/faculty/srd.html

The Protein Data Bank: http://www.rcsb.org/pdb

SUPPLEMENTARY INFORMATION

See online article: S1 (box)

Access to this links box is available online.